Published in Applied Physics Letters, 106, 163505 -1/5, 2015
which should be used for any reference to this work

Aging studies on micro-fabricated alkali buffer-gas cells for miniature atomic clocks

S. Abdullah, C. Affolderbach, F. Gruet, and G. Mileti[a)]
Laboratoire Temps-Fréquence, Institut de Physique, Université de Neuchâtel, Neuchâtel CH-2000, Switzerland

We report an aging study on micro-fabricated alkali vapor cells using neon as a buffer gas. An experimental atomic clock setup is used to measure the cell's intrinsic frequency, by recording the clock frequency shift at different light intensities and extrapolating to zero intensity. We find a drift of the cell's intrinsic frequency of $(-5.2 \pm 0.6) \times 10^{-11}$/day and quantify deterministic variations in sources of clock frequency shifts due to the major physical effects to identify the most probable cause of the drift. The measured drift is one order of magnitude stronger than the total frequency variations expected from clock parameter variations and corresponds to a slow reduction of buffer gas pressure inside the cell, which is compatible with the hypothesis of loss of Ne gas from the cell due to its permeation through the cell windows. A negative drift on the intrinsic cell frequency is reproducible for another cell of the same type. Based on the Ne permeation model and the measured cell frequency drift, we determine the permeation constant of Ne through borosilicate glass as $(5.7 \pm 0.7) \times 10^{-22}$ m^2 s^{-1} Pa^{-1} at 81 °C. We propose this method based on frequency metrology in an alkali vapor cell atomic clock setup based on coherent population trapping for measuring permeation constants of inert gases.

Micro-fabricated alkali-atom vapor cells with volumes of few mm^3 are of interest for applications in instruments such as miniature atomic magnetometers,[1] gyroscopes,[2] imaging of microwave fields,[3] and atomic clocks.[4] Particular applications like Chip Scale Atomic Clocks[5] (CSAC) based on Coherent Population Trapping (CPT)[6] were first reported by NIST.[7,8] Subsequent studies on the long term clock fre-quency drifts by NIST[9,10] and Symmetricom[11] identified possible sources of the frequency drifts and suggested rem-edies. Considerable work has been reported on the fabrica-tion[12] and characterization[3] of miniature vapor cells, but only few studies addressed the long term frequency drifts in miniature atomic clocks induced specifically by the vapor cell itself. Certain studies[9,10] suggest that the buffer gas pres-sure change inside the vapor cell causes the long term clock frequency drift; however, no quantitative treatment of the buffer gas pressure change nor a systematic evaluation of other contributions was given. The concept of the buffer gas pressure change as possible cause of the in-orbit frequency equilibration of space clocks has been studied by Camparo *et al.*,[13,14] in view of the He buffer gas permeation through the cell walls. The quantitative treatment of the He buffer gas permeation through the cell walls by Camparo[13] points at the importance of the buffer gas pressure change as one of the crucial parameters to be considered, but the observed clock frequency drift could not be explained by this process. Note that all these studies[9–11,13,14] were performed in clock operation conditions, i.e., under conditions where the light shift, in general, is non-zero and can be a dominant contributor to the clock frequency drift. Furthermore, they could neither link the observed clock frequency drift to the intrinsic properties of the vapor cell used nor quantify the clock frequency aging in terms of the buffer gas pressure evolution inside the vapor cell.

Only few authors have addressed explicitly the aging or drift of the intrinsic frequency of the vapor cell alone, i.e., when other sources of drift arising from the clock system operation are excluded, that could be caused by a change of buffer-gas pressure. For instance, Kazantsev *et al.*[15] employed measuring the clock frequency shifts for precision measurement of buffer gas pressure. Recently, Hasegawa *et al.*[16,17] studied aging in micro-fabricated Cs-Ne vapor cells using CPT spectroscopy of the Cs clock transition ($6S_{1/2}$, $F = 3$, $m_F = 0 \leftrightarrow 6S_{1/2}$, $F = 4$, $m_F = 0$), by extrapolating the clock frequency to zero light intensity. However, no drift of the clock resonance frequency could be shown. Straessle *et al.*[18] discussed permeation of Nitrogen buffer gas into their Rb micro-cells to assess the hermiticity of micro-cells.

The motivation of our present study is to identify and quantitatively analyze the possible sources of clock frequency drift in miniature atomic clocks, induced by potential aging of the miniature vapor cells, such as, e.g., a slow change of buffer gas pressure. We identify the sources of clock frequency variations which in standard clock operation conditions mask the frequency drifts due to aging of the cell. Extrapolation of the clock frequency to zero light level is used to record the *intrinsic cell frequency* that is unaffected by light-shift effects. Repeating the measurements over time permits to observe the aging of this intrinsic cell frequency, which is crucial for the long-term stability of the atomic clock.

Permeation of noble gases, e.g., Ne, through the intact solid cell walls[19] is a known process that can cause a change

[a)]Author to whom correspondence should be addressed. Electronic mail: gaetano.mileti@unine.ch

TABLE I. Comparison of permeation constants K for He and Ne from the literature, and predicted resulting valued for τ, L, and intrinsic cell frequency drift for the microfabricated cell under study, at 81 °C.

Permeation system	K ($m^2\,s^{-1}\,Pa^{-1}$)	L (mbar·l/s)	τ (days)	Initial frequency drift (day^{-1})
He through Pyrex 7740 (Ref. 20)	6.5×10^{-19}	2.0×10^{-9a}	62[a]	$+9.6\times10^{-12a}$
Ne through silica (Ref. 22)	1.9×10^{-21}	5.6×10^{-12a}	2.1×10^{4a}	-1.7×10^{-10a}
Ne through Pyrex 7740 (Ref. 24)	1.06×10^{-22}	3.1×10^{-13a}	3.8×10^{5a}	-9.6×10^{-12a}

[a]Values calculated from reference data for K.

of buffer-gas pressure in a vapor cell. The evolution of the buffer gas pressure P_{in} (t) inside the cell can be described in terms of a permeation rate L (units of mbar·l/s, in analogy to a leak rate) for the buffer gas volumetric flow into or out of the cell by[18]

$$P_{in}(t) = P_{ext} - (P_{ext} - P_{in})e^{\frac{-Lt}{VP_{ref}}} = P_{ext} - (P_{ext} - P_{in})e^{\frac{-t}{\tau}}. \quad (1)$$

Here $P_{ext} = 0.018$ mbar is the partial pressure of Ne in the atmosphere, $P_{in} = P_{in}(t = 0)$, V is the volume of the vapor cell (10 μl in our case), and $P_{ref} = 1013$ mbar is the atmospheric reference pressure. The process of Eq. (1) has the time constant of[18]

$$\tau = \frac{VP_{ref}}{L}. \quad (2)$$

The permeation rate L through a membrane of area A and thickness d is expressed in terms of the permeation constant K ($m^2\,s^{-1}\,Pa^{-1}$) a s [18]

$$L = \frac{KA}{d}P_{ref}^2. \quad (3)$$

Permeation of gases such as He, Ne, Ar, and N_2 through different materials has been studied by several authors,[19–23] with He as the smallest molecule showing the strongest permeation. Permeation of He through silica and borosilicate glasses was reported by Norton[19] and Harding[20] for the temperature range of −80 °C to 700 °C and by Altemose[21] for 100 °C to 600 °C. Ne permeation was studied by Wortmann and Shackelford[22] for vitreous silica glasses at 0 °C t o 5 0 °C, by Kanezashi *et al.*[23] for silica glass at 300 °C to 600 °C, and by Shelby[24] for borosilicate glasses at 200 °C to 560 °C. Recently, Zameroski *et al.*[25] have discussed the impact of He permeation into an alkali vapor cell on their measurement of collisional shift rates of Cs optical transitions, using data from Altemose.[21] To summarize, most of these works reported on the permeation of He through different glasses at elevated temperature ranges where permeation is enhanced,[19] while no study has been reported so far on the impact of Ne permeation through borosilicate glass in atomic clock applications. Table I lists permeation constants for He or Ne from literature. Expected permeation rates, time con-stants, and initial linear drift of intrinsic cell frequency due to permeation are given, calculated for the microfabricated Cs-Ne cell under study (see below), using P_{in} = 60 mbar and the Ne pressure shift coefficient of 530 Hz/mbar.[26] Because K for permeation of both He and Ne through Si[27] is several orders of magnitude smaller than through borosilicate glass,[18,24] one can neglect the Si parts of the cell here and treat τ of Eq. (2) applying to the cell's borofloat windows only. Note that because for our Ne buffer gas cells $P_{in} \gg P_{ext}$, a n e g - ative drift of the intrinsic cell frequency is expected.

The Cs micro-cells studied (see Fig. 1(b)) are similar to those described by Hasegawa *et al.*[16,17] The cells are composed of a 1.4 mm thick Si wafer, closed on both sides by a 0.5 mm thick borofloat33 glass[28] plate using anodic bonding.[29] The cells have a two chamber design, with one chamber housing a Cs dispenser and a separate chamber of 2 mm diameter for atom interrogation. After cell sealing, atomic Cs is released from the dispenser by local heating with a laser beam, using the post-activation process reported by Nieradko *et al.*[30] The cells also contain pure Ne buffer gas that shows a nonlinear temperature dependence of the Cs clock transition frequency, resulting in suppressed tempera-ture sensitivity close to the inversion temperature of 81 °C.[26,31]

We measure the intrinsic frequency of the Cs-Ne vapor cells using an experimental atomic clock,[31,32] see Fig. 1(a). A distributed feedback (DFB) diode laser emits light at 894 which is frequency modulated by a fiber coupled Electro Optic Modulator (EOM) driven by a frequency synthesizer at ≈4.6 GHz (half the Cs ground-state splitting), resulting in a phase modulation index of M = 1.53 for the optical spectrum. CPT resonances are excited with the two first-order modulation sidebands, of right-handed circular polarization, coupling the $|F_g = 3, m_F = 0>$ and $|F_g = 4, m_F = 0>$ states to

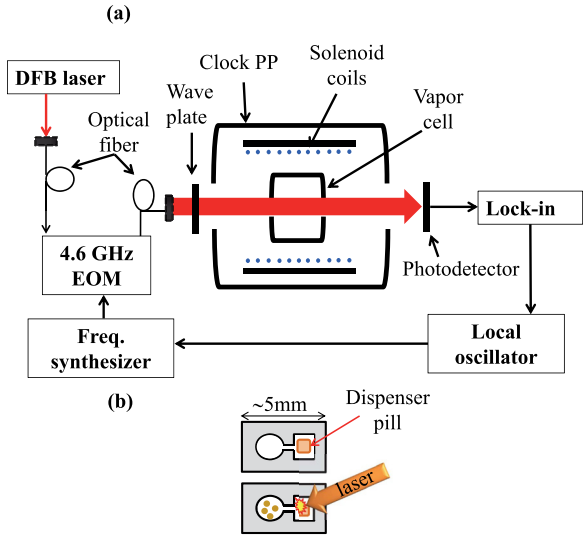

FIG. 1. (a) Schematic setup of the CPT atomic clock. (b) Schematic of the two chamber cell design. The circular chamber is the optical interrogation chamber, and the Cs dispenser pill is shown along with a laser used for releasing the Cs vapors through post activation.

$|F_e = 4\ m_F = 1\rangle$ on the Cs D1 line, with a total optical intensity of 0.5 mW/cm^2. We test two similar vapor cells, samples 1 and 2, with Ne buffer gas pressures of 62 and 77 mbar, respectively. The vapor cell under test is housed in the clock physics package, where it is held at a temperature of 81 °C (inversion temperature of Cs clock transition for Ne buffer gas[31]), and a DC magnetic field of 5.8 μT is applied to lift the Zeeman degeneracy of the Cs ground states. We refer to these experimental conditions as the clock operation conditions.

Fig. 2 shows a typical CPT resonance, with a line width of 6.7 kHz and a contrast of 0.62%. For measuring the clock frequency, we close the clock loop and use a phase comparator to measure the local oscillator (LO) frequency against a 5 MHz H-maser reference (frequency stability of $\approx 10^{-15}$ at 1000 s, long-term drift of 5×10^{-15}/day).

We now quantify different sources of instability in clock operating conditions, evaluated as Allan deviation at one day of integration time here to obtain upper limits on the deterministic long-term changes. The intensity light shift coefficient α[32] is given by the slope of the clock frequency as a function of the light intensity. With $\alpha = 300$ Hz·cm^2/mW and a fractional intensity instability of the DFB laser, $\sigma_{\Delta I_L/I_L} = 4.5 \times 10^{-3}$ at one day, the clock fractional frequency instability at one day induced by the intensity light shift is obtained as[31]

$$\sigma_\alpha(\tau) = \frac{I.\sigma_{\Delta I_L/I_L}.\alpha}{\nu_{cs}} = (9.7 \pm 1.4) \times 10^{-11}. \qquad (4)$$

Similarly, we use a frequency light shift coefficient β of -644 mHz/MHz (Ref. 32) and estimate[33] the fractional frequency instability of the DFB laser, $\sigma_{\Delta\nu_L/\nu_L} \approx 7 \times 10^{-9}$ at one day, for laser frequency locking to the buffer-gas broad-ened Cs D1 absorption lines. The fractional clock frequency instability at one day induced by the frequency light shift is then[31]

$$\sigma_\beta(\tau) = \frac{\nu.\sigma_{\Delta\nu_L/\nu_L}.\beta}{\nu_{cs}} = (1.2 \pm 0.1) \times 10^{-10}. \qquad (5)$$

The second-order Zeeman effect induces a clock frequency offset of +1.4 Hz, calculated from the second-order Zeeman coefficient[34] of $K_0 = 427 \times 10^8$ Hz/T^2, and the total magnetic field at cell location (including applied C-field, geomagnetic field, effect of magnetic shields, etc.) measured on magnetically sensitive Zeeman transitions. Repeated measurement of the magnetic field over the study duration (see Fig. 3) yields the

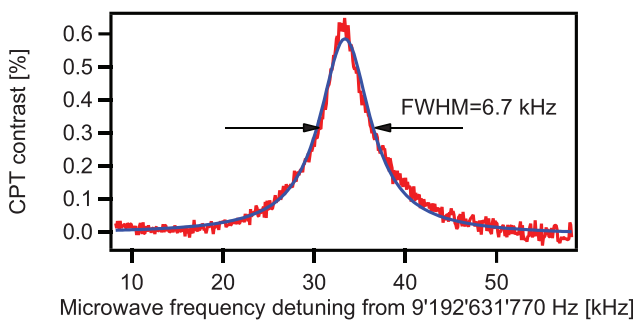

FIG. 2. CPT signal contrast as a function of the microwave detuning from the unperturbed Cs ground-state splitting, recorded under clock operation conditions. Red line: experimental data, and blue line: Lorentzian fit.

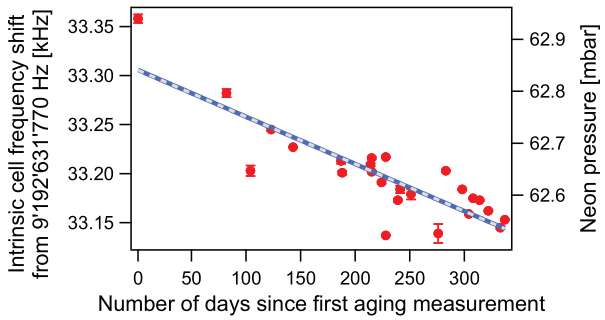

FIG. 3. Temporal evolution of the intrinsic cell frequency and buffer gas pres-sure as a function of time for cell sample 1. Red circles: experimental data. Solid blue line: exponential fit from Eq. (1). Dashed grey line: linear fit.

clock fractional frequency variations due to the second order Zeeman effect of $(8.7 \pm 2.1) \times 10^{-14}$ at one day, which includes the deterministic variations of external magnetic fields here. Using the first-order temperature coefficient of $(4.8 \pm 0.5) \times 10^{-10}$/K measured for the vapor cell and an estimated 10 mK of cell temperature variation at one day,[35,36] we calculate a temperature-induced fractional clock frequency instability of $(5.1 \pm 0.2) \times 10^{-12}$ at one day (long-term deterministic drifts from potential aging of key electronic components are estimated to be ten times smaller). The impact of the cell barometric effect[37] on the clock fre-quency instability depends on the environmental pressure variation, measured at one day as 5×10^{-3} mbar.[38] By scal-ing Riley's data[37] to our cell, we find a barometric sensitivity of our cell of 5×10^{-6} Hz/mbar and a corresponding clock frequency instability of $(2.4 \pm 1.0) \times 10^{-15}$ at one day.

Table II summarizes the upper limits on the deterministic variations in the clock frequency shifts, in terms of $\sigma(\tau)$ a t $\tau =$ 1 day. The total frequency variation is calculated as $(2.2 \pm 0.5) \times 10^{-10}$/day, with the light-shift as dominating con-tribution. The measured clock frequency stability reaches 3×10^{-11} at 100 s and 2.7×10^{-10} at one day, in close agree-ment with the total clock frequency variation from Table II. Clock frequency drifts recorded over several days are around 1×10^{-10}/day, also consistent with the upper limits of Table II.

In order to avoid the dominant instability contribution due to the light shift, we periodically determine the intrinsic cell frequency by recording the clock frequency for different light intensities and extrapolating to zero light intensity. The temporal variation in the statistical uncertainty from this extrapolation is computed to be $(4.2 \pm 1.1) \times 10^{-13}$/day. We

TABLE II. Upper limits on the long-term deterministic variations in sources of clock frequency shifts.

Source of frequency shift	$\sigma(\tau)$ in clock operation conditions (at 1 day)	$\sigma(\tau)$ in zero-light extrapolation (at 1 day)
Frequency light shift	$(1.2 \pm 0.1) \times 10^{-10}$	$(4.2 \pm 1.1) \times 10^{-13}$
Intensity light shift	$(9.7 \pm 1.4) \times 10^{-11}$	
Cell temperature shift	$(5.1 \pm 0.2) \times 10^{-12}$	$(5.1 \pm 0.2) \times 10^{-12}$
Cell barometric shift	$(2.4 \pm 1.0) \times 10^{-15}$	$(2.4 \pm 1.0) \times 10^{-15}$
Second order Zeeman shift	$(8.7 \pm 2.1) \times 10^{-14}$	$(8.7 \pm 2.1) \times 10^{-14}$
Total variation	$(2.2 \pm 0.24) \times 10^{-10}$	$(5.6 \pm 0.2) \times 10^{-12}$

TABLE III. Time constant and linear drift of intrinsic cell frequency from Fig. 3, and resulting permeation rates L and permeation constants K, for the micro-fabricated cell under study at 81 °C.

Permeation system	K ($m^2\ s^{-1} Pa^{-1}$)	L (mbar·l/s)	τ (days)	Frequency drift (day $^{-1}$)
Ne through borofloat33	$(5.7 \pm 0.7) \times 10^{-22a}$	$(1.7 \pm 0.2) \times 10^{-12a}$	$69\,700 \pm 8\,500$	$(-5.2 \pm 0.6) \times 10^{-11}$

[a]Values calculated from τ from Fig. 3.

take this value as estimate of the residual clock frequency variation due to light-shifts in zero-light extrapolation and find a total frequency variation of $(5.6 \pm 0.2) \times 10^{-12}$ at one day due to the variation of physical parameters in this case.

The temporal evolution of the measured zero-light extrapolated clock frequency (i.e., the cell's intrinsic frequency) is shown in Fig. 3, for a period of 11 months, and shows a linear drift of $(-5.2 \pm 0.6) \times 10^{-11}$/day, in agreement with expectations from Table I. This drift is one order of magnitude lower than the total frequency variation in clock operating conditions and thus cannot be observed in this mode. But it is also one order of magnitude higher than the expected maximum clock frequency variations in zero-light extrapolation from Table II, so we conclude that the processes considered in Table II cannot explain the intrinsic cell frequency drift observed and attribute it to a change in the cell's gas pressure.

Using the Ne pressure shift coefficient of 530 Hz/mbar (Ref. 26) for the clock transition, the linear drift of the intrinsic cell frequency in Fig. 3 corresponds to a change in buffer gas pressure of (-0.9 ± 0.1) μbar/day in cell sample 1. We exclude Ne absorption by the Cs dispenser,[16] permeation of gases with negative pressure coefficients like Ar into the cell (permeation rates more than five orders of magnitude smaller than Ne for a borosilicate glass[19]), and gas losses by micro-leaks (that should result in a positive frequency drift due to intake of atmospheric N_2), and therefore attribute the decrease in Ne pressure to Ne permeation through cell win-dows out of the cell.

Fitting the data of Fig. 3 with the permeation model of Eq. (1), we find a time constant of $\tau = (69\,700 \pm 8500)$ days. Note that due to the long time constant, the exponential behavior appears close to linear on the time scale of Fig. 3. From Eqs. (2) and (3), this corresponds to a permeation rate of $(1.7 \pm 0.2) \times 10^{-12}$ mbar·l/s and a permeation constant of $(5.7 \pm 0.7) \times 10^{-22}\ m^2\ s^{-1}\ Pa^{-1}$ for Ne permeation through borofloat33, see Table III. Using Eq. (1), the initial change of buffer gas pressure is found as (-0.9 ± 0.1) μbar/day, in good agreement with the pressure change of (-0.9 ± 0.1) μbar/day inferred from the linear drift of intrinsic cell frequency of $(-5.2 \pm 0.6) \times 10^{-11}$/day.

The cell aging measurements started one month after cell sealing and activation, and He permeation into the cell can affect its intrinsic frequency. Using the data for He permeation[20] from Table I, 5.3×10^{-3} mbar atmospheric He partial pressure, and the fractional frequency sensitivity of 9×10^{-8}/mbar,[34] the maximum total clock frequency shift caused by He permeation until the end of the equilibration process is +4 Hz, which is negligible compared to the −140 Hz overall clock frequency change observed in Fig. 3.

TABLE IV. Comparison of measured intrinsic cell frequency drifts for different vapor cells.

Cell sample	P_{Ne} (mbar)	T_{cell} (°C)	Intrinsic cell frequency drift (/day)
1	62	81	$(-5.2 \pm 0.6) \times 10^{-11}$
2	77	150	$(-4.5 \pm 0.2) \times 10^{-10}$

An accelerated aging study was performed on an addi-tional vapor cell (sample 2) of same type held at (150 ± 10) °C for 54 days. At this temperature, one expects[24] K(150 °C) ≈ $(10 \pm 2.5) \times$ K(81 °C) ≈ $(5.6 \pm 1.4) \times 10^{-21}\ m^2\ s^{-1}\ Pa^{-1}$ (using K(81 °C) from Table III) and an intrinsic cell fre-quency drift of $(-6.3 \pm 1.6) \times 10^{-10}$/day. A two-point mea-surement of the intrinsic cell frequency (performed before and after accelerated aging) yields a drift of $(-4.5 \pm 0.2) \times 10^{-10}$/day, see Table IV, reasonably close to the expected value.

In conclusion, we presented a method for studying the aging behavior of micro-fabricated Cs-Ne vapor cells, by repeat-edly measuring the intrinsic cell frequency with an atomic clock setup. For both cell samples studied, we find a negative fre-quency drift, one order of magnitude above the measurement uncertainty. This observation can be explained by permeation of the Ne buffer-gas out of the cell through the glass windows, with a permeation constant K= $(5.7 \pm 0.7) \times 10^{-22}\ m^2\ s^{-1}\ Pa^{-1}$ for Ne through Borofloat33 glass at 81 °C. The validity of this process could further be confirmed by conducting the aging study inside a chamber with high Ne pressure, where a positive drift on the intrinsic clock frequency is expected. Absorption of Ne by the Cs dispenser is excluded here,[16] which could be confirmed by conducting our aging study on micro-fabricated cells without Cs dispensers. Our results are relevant for assessing the long-term stability of miniature atomic clocks based on this cell technology. The experimental method can also be used to determine permeation rates and permeation constants for gases through different cell materials.

The authors gratefully acknowledge fruitful discussions with M. Pellaton (Université de Neuchâtel) and S. Karlen (CSEM SA, Neuchâtel, Switzerland) on buffer gas permeation, Y. Pétremand (CSEM) for providing the vapor cells, and D. Varidel (Université de Neuchâtel) for support with the H-maser reference. This work was funded by the Swiss National Science Foundation (FNS) and co-financed by the Swiss Commission for Technology and Innovation (CTI).

[1]T. Scholtes, V. Schultze, R. IJsselsteijn, S. Woetzel, and H.-G. Meyer, Opt. Express **20**, 29217 (2012).
[2]E. Donley, J. Long, T. Liebisch, E. Hodby, T. Fisher, and J. Kitching, Phys. Rev. A **79**, 013420 (2009).
[3]A. Horsley, G. Du, M. Pellaton, C. Affolderbach, G. Mileti, and P. Treutlein, Phys. Rev. A **88**, 063407 (2013).

[4]M. Pellaton, C. Affolderbach, Y. P´etremand, N. de Rooij, and G. Mileti, Phys. Scr. **T149**, 014013 (2012).
[5]S. Knappe, "Emerging topics: MEMS atomic clocks," in *Comprehensive Microsystems*, edited by Y. Gianchandani, O. Tabata, and H. Zappe (Elsevier, The Netherlands, 2007).
[6]G. Alzetta, A. Gozzini, L. Moi, and G. Orriols, Nuovo Cimento **36**, 5 (1976).
[7]J. Kitching, L. Hollberg, S. Knappe, and R. Wynands, Electron. Lett. **37**, 1449 (2001).
[8]S. Knappe, V. Shah, P. Schwindt, L. Hollberg, J. Kitching, L. Liew, and J. Moreland, Appl. Phys. Lett. **85**, 1460 (2004).
[9]S. Knappe, V. Gerginov, P. Schwindt, V. Shah, H. G. Robinson, L. Hollberg, and J. Kitching, Opt. Lett. **30**, 2351 (2005).
[10]J. Kitching, S. Knappe, L. Liew, J. Moreland, P. Schwindt, V. Shah, V. Gerginov, and L. Hollberg, Metrologia **42**, S100 (2005).
[11]R. Lutwak, J. Deng, W. Riley, M. Varghes e , J . L e b l a n c , G . T e p o l t , M . M e s c h e r , D . K . S e r k l a n d , K . M . G e i b , a n d G . M . P eake, in 36th Annual Precision Time and Time Interval
[12]Meeting, Washington, DC, 7–9 December 2004.
A. Douahi, A. Douahi, L. Nieradko, J. C. Beugnot, J. Dziuban, H. Maillote, S. Gu´erandel, M. Moraja, C. Gorecki, and V. Giordano, Electron. Lett. **43**,
[13]279 (2007).
J. Camparo, C. Klimcak, and S. Herbulock, IEEE Trans. Instrum. Meas.
[14]**50**, 1873 (2005).
J. Camparo and C. Klimcak, in 39th Annual Precision Time and Time
[15]Interval Meeting, California, 26–29 November 2007.
S. A. Kazantsev, G. M. Smirnova, and V. I. Khutorshchikov, Opt.
[16]Spectrosc. **80**(1), 10 (1996).
M. Hasegawa, R. K. Chutani, C. Gorecki, R. Boudot, P. Dziuban, V.
[17]Giordano, S. Clatot, and L. Mauri, Sens. Actuators, A **167**, 594 (2011). M. Hasegawa, R. K. Chutani, R. Boudot, L. Mauri, C. Gorecki, X. Liu, and
[18]N. Passily, J. Micromech. Microeng. **23**, 055022 (2013).
R. Straessle, M. Pellaton, C. Affolderbach, Y. Petremand, D. Briand, G. Mileti, and N. F. de Rooij, J. Appl. Phys. **113**, 064501 (2013).
[19]F. J. Norton, J. Appl. Phys. **28**, 34 (1957).
[20]G. L. Harding, Sol. Energy Mater. **5**, 141 (1981).
[21]V. O. Altemose, J. Appl. Phys. **32**, 1309 (1961).
[22]R. S. Wortman and J. F. Shackelford, J. Non-Cryst. Solids **25**, 280 (1990).
[23]M. Kanezashi, T. Sasaki, H. Tawarayama, H. Nagasawa, T. Yoshioka, K. Ito, and T. Tsuru, J. Phys. Chem. C **118**, 20323 (2014).
[24]J. E. Shelby, J. Appl. Phys. **45**, 2146 (1974).
[25]N. D. Zameroski, G. D. Hager, C. J. Erickson, and J. H. Burke, J. Phys. B: At., Mol. Opt. Phys. **47**, 225205 (2014).
[26]O. Kozlova, S. Gu´erandel, and E. de Clercq, Phys. Rev. A **83**, 062714 (2011).
[27]A. Van Wieringen and N. Warmoltz, Physica **22**, 849 (1956).
[28]Schott borofloat33 datasheet, Schott technical glass solutions GmbH, Jena, Germany, see http://www.schott.com/borofloat.
[29]Y. P´etremand, C. Affolderbach, R. Straessle, M. Pellaton, D. Briand, G. Mileti, and N. F. de Rooij, J. Micromech. Microeng. **22**, 025013 (2012). L.
[30]Nieradko, C. Gorecki, A. Douahi, V. Giordano, and J. C. Beugnot, J. Micro/Nanolithogr., MEMS, MOEMS **7**, 033013 (2008).
[31]D. Miletic, Ph.D. thesis, Universite´ de Neuchˆatel, 2013.
[32]D. Miletic, C. Affolderbach, M. Hasegawa, R. Boudot, C. Gorecki, and G. Mileti, Appl. Phys. B **109**, 89 (2012).
[33]F. Gruet, M. Pellaton, C. Affolderbach, T. Bandi, R. Matthey, and G. Mileti, in Proceedings of the International Conference on Space Optics, Ajaccio, 9–12 October 2012.
[34]J. Vanier and C. Audoin, *Quantum Physics of Atomic Frequency Standards* (Hilger, Philadelphia, 1989).
[35]T. Bandi, Ph.D thesis, Universit´e de Neuchˆatel, 2013.
[36]M. Pellaton, Ph.D thesis, Universit´e de Neuchˆatel, 2014.
[37]W. J. Riley, IEEE Trans. Ultrason. Ferroelectr. Freq. Control. **39**, 232 (1992).
[38]Environmental pressure and temperature data were provided by Meteoswiss, the Swiss Federal Office of Meteorology and Climatology.